

Symbolic Execution of Toffoli-Hadamard Quantum Circuits

Jacques Carette
McMaster University
Hamilton, ON, Canada

Gerardo Ortiz
Indiana University
Bloomington, IN, USA

Amr Sabry
Indiana University
Bloomington, IN, USA

ACM Reference Format:

Jacques Carette, Gerardo Ortiz, and Amr Sabry. 2022. Symbolic Execution of Toffoli-Hadamard Quantum Circuits. In *Proceedings of ACM Conference (Conference'17)*. ACM, New York, NY, USA, 10 pages. <https://doi.org/10.1145/nnnnnnn.nnnnnnn>

1 Introduction

The general state of a quantum bit (qubit) is mathematically modeled using an equation parameterized by two angles θ and ϕ as follows:

$$\cos \frac{\theta}{2} |0\rangle + e^{i\phi} \sin \frac{\theta}{2} |1\rangle$$

The description models the fact that the qubit is in a superposition of false $|0\rangle$ and true $|1\rangle$. The angle θ determines the relative amplitudes of false and true and the angle ϕ determines the relative phase between them. A particular case when $\theta = \pi/2$ and $\phi = 0$ is ubiquitous in quantum algorithms. In those cases, the general representation reduces to:

$$1/\sqrt{2}(|0\rangle + |1\rangle)$$

which represents a qubit in an equal superposition of false and true.

The reason this particular case is distinguished is because a rather common template for quantum algorithms is to start with qubits initialized to $|0\rangle$ and immediately apply a Hadamard H transformation whose action is $|0\rangle \mapsto 1/\sqrt{2}(|0\rangle + |1\rangle)$. This superposition is then further manipulated depending on the algorithm in question.

Our observation is that a qubit in the special superposition $1/\sqrt{2}(|0\rangle + |1\rangle)$ is, computationally speaking, indistinguishable from a symbolic boolean variable with an unknown value in the same sense used in symbolic evaluation of classical programs. First, the superposition is not observable. The only way to observe the qubit is via a measurement

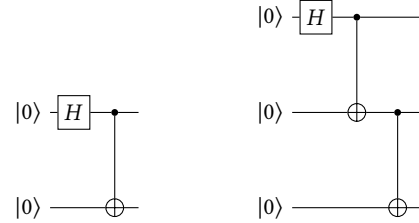


Figure 1. Bell and GHZ States

which collapses the state to be either false or true with equal probability. Second, and more significantly, this remarkably simple observation is quite robust even in the presence of multiple, possibly entangled, qubits.

To see this, consider the conventional quantum circuits for creating the maximally entangled Bell and GHZ states in Fig. 11. On the left, the circuit generates the Bell state $(1/\sqrt{2})(|00\rangle + |11\rangle)$ as follows. First the state evolves from $|00\rangle$ to $(1/\sqrt{2})(|00\rangle + |10\rangle)$. Then we apply the cx-gate whose action is to negate the second qubit when the first one is true. By using the symbol x for $H|0\rangle$, the input to the cx-gate is $|x0\rangle$. A simple case analysis shows that the action of cx-gate on inputs $|xy\rangle$ is $|x(x \oplus y)\rangle$ where \oplus is the exclusive-or boolean operation. In other words, the cx-gate transforms $|x0\rangle$ to $|xx\rangle$. Since any measurement of the Bell state must produce either 00 or 11, by producing a symbolic state that shares the same name in two positions, we have accurately represented the entangled Bell state. Similarly, for the GHZ circuit on the right of Fig. 11, the state after the Hadamard gate is $|x00\rangle$ which evolves to $|xx0\rangle$ and then to $|xxx\rangle$ again accurately capturing the entanglement correlations.

The introduction to symbolic variables opens a host a new exciting possibilities. Consider again the Bell circuit in Fig. 9a with an arbitrary initial value for the second qubit. The right subfigure Fig. 9b removes the explicit use of $H|0\rangle$ and replaces the top qubit with another symbolic variable. Because quantum circuits are reversible, we can, at this point, “partially evaluate” the circuit under various regimes. For example, we can set $y_1 = 0$ and $y_2 = 1$ and ask about values of x_1 and x_2 that would be consistent with this setting. We can calculate backwards from $|x_21\rangle$ as follows. The state evolves to $|x_2(1 \oplus x_2)\rangle$ which can be reconciled with the initial conditions yielding the constraints $x_1 = x_2$ and $1 \oplus x_2 = 0$ whose solutions are $x_1 = x_2 = 1$.

Permission to make digital or hard copies of all or part of this work for personal or classroom use is granted without fee provided that copies are not made or distributed for profit or commercial advantage and that copies bear this notice and the full citation on the first page. Copyrights for components of this work owned by others than ACM must be honored. Abstracting with credit is permitted. To copy otherwise, to republish, to post on servers or to redistribute to lists, requires prior specific permission and/or a fee. Request permissions from permissions@acm.org.

Conference'17, July 2017, Washington, DC, USA

© 2022 Association for Computing Machinery.

ACM ISBN 978-x-xxxx-xxxx-x/YY/MM. . \$15.00

<https://doi.org/10.1145/nnnnnnn.nnnnnnn>



Figure 2. A conventional quantum circuit for generating a Bell state (a); its classical symbolic variant.

2 Circuits and Boolean Functions

TODO: Make sure to document the “Circuit Abstraction” that’s in comments at the top of `Circuits.hs`, along with the picture. Either here or ensure it occurs before.

Algebraic Normal Form (ANF). The semantics of a generalized Toffoli gate with n control qubits: a_{n_1}, \dots, c_0 and one target qubit b is $b \oplus \bigwedge_i a_i$, the exclusive-or of the target b with the conjunction of all the control qubits. That is precisely the definition of the algebraic normal form of boolean expressions. We note that circuits that only use x and cx -gates never generate any conjunctions and hence lead to formulae that efficiently solvable classically [30, 34].

3 Symbolic Evaluation of Circuits

For quantum circuits over H , CCX restrict to $|0\rangle$ inputs; look at state after the initial group of H gates

classical wires treated as known
superpositions $|0\rangle + |1\rangle$ treated as symbols x
run circuit with known values and symbol for superpositions

4 Design and Implementation

Our exposition of the design and implementation of our system will follow Parnas’ advice on *faking it* [?]: a reconstruction of the requirements as we should have had them if we’d been all-knowing, and a design that fits those requirements. The version history in our github repository can be inspected for anyone who wants to see our actual path.

As we experimented with the idea of partial evaluation and symbolic execution of circuits, we ended up writing a lot of variants of essentially the same code, but with minor differences in representation. From these early experiments, we could see the major variation points:

- representation of *boolean values* and *boolean functions*,
- representation of ANF,
- representation of circuits.

We also wanted to write out circuits only once, and have them be valid across these representation changes.

A number of our examples involve arbitrary boolean functions (given as black boxes at “compile time”) for which we want to, offline, generate an equivalent reversible circuit. In other words for $f : \mathbb{B}^n \rightarrow \mathbb{B}$, we wish to generate the circuit for $g : \mathbb{B}^{n+1} \rightarrow \mathbb{B}^{n+1}$ such that for $\bar{x} : \mathbb{B}^n$, then $g(\bar{x}, y) = (\bar{x}, y \oplus f(\bar{x}))$.

This leads us to the requirements our code must fulfill.

4.1 Requirements

We need to be able to deal with the following variabilities:

1. multiple representations of *boolean values*,
2. multiple representations of *boolean formulas*,
3. different evaluation means (directly and symbolically),

It must also be possible to implement the following:

4. a reusable representation of circuits composed of generalized Toffoli gates,
5. a reusable representation of the inputs, outputs and ancillas associated to a circuit,
6. a *synthesis* algorithm for circuits implementing a certain boolean function,
7. a reusable library of circuits (such as Deutsch, Deutsch-Jozsa, Bernstein-Vazirani, Simon, Grover, and Shor).

From those, we can make a set of design choices that drive the eventual solution.

We eventually want some non-functional characteristics to hold:

8. evaluation of reasonably-sized circuits should be relatively efficient.

4.2 Design

To meet the first requirement, we use *finally tagless* [?] to encode a *language of values*:

```
class (Show v, Enum v) => Value v where
  zero :: v
  one  :: v
  snot :: v -> v
  sand :: v -> v -> v
  sxor :: v -> v -> v

-- has a default implementation
snand :: [v] -> v -- n-ary and
snand = foldr sand one
```

which is then implemented 4 times, once for `Bool` and then multiple times for different symbolic variations. As a side-effect, this gives us requirement 3 “for free” if we can write a sufficiently polymorphic evaluator (which we will present below).

Unlike for value representation which can be computed from context, we want to explicitly choose formula representation (requirement 2) ourselves. Thus we use an explicit record instead of an implicit dictionary:

```
data FormulaRepr f r = FR
  { fromVar   :: r -> f
  , fromVars  :: Int -> r -> [ f ]
  }
```

The main methods are about *variable representation* r and how to insert them into the current *formula representation* f , singly or n at once.

A Generalized Toffoli gates can be represented by a list of representation of value accessors br (short for boolean representation) along with a list of *controls* that tell us whether to use the bit directly or negated, along with which value will potentially be flipped. The implementation of very common gates (negation and controlled not) are also shown.

```
data GToffoli br = GToffoli [Bool] [br] br
```

```
xop :: br -> GToffoli br
xop = GToffoli [] []
```

```
cx :: br -> br -> GToffoli br
cx a = GToffoli [True] [a]
```

The core of a circuit (requirement 4) is then implemented as a sequence of these (where `Seq` is from `Data.Sequence`).

```
type OP br = Seq (GToffoli br)
```

Mainly for efficiency reasons, we model circuits as manipulating *locations holding values* rather than directly acting on values. We use `STRefs` (aliased to `Var`) for that purpose. Putting this together with the model of circuits of `??`, we get

```
data Circuit s v = Circuit
  { op      :: OP (Var s v)
  , xs      :: [Var s v]
  , ancillaIns :: [Var s v]
  , ancillaOuts :: [Var s v]
  , ancillaVals :: [v]
  }
```

which lets us achieve requirement 5.

For requirement 6, we implement a straightforward version of the algorithm of [?]. Our implementation is *language agnostic*, in other words it works via the `Value` interface, so that the resulting circuits are all of type `OP br` for a free representation br . As circuit synthesis is only done for generating examples, we are not worried about its efficiency.

The arithmetic circuit generators are also based on classical algorithms, and are not optimized in any way, neither for running time nor for gate count. Neither are the code for the classical quantum algorithms. They are, however, representation polymorphic.

Above, we said we had 3 different symbolic evaluators. These were not driven by having different levels of *precision* but rather by requirement 8, efficiency. Our first evaluator (`FormASList`) uses xor-lists of and-lists of literals (as strings, i.e. " $x0$ ", " $x1$ ", ... in lexicographical order of the wires). ANF is then easy: and-lists are sorted, and duplicates removed.

Xor-lists are sorted, grouped, even length lists are removed, and then made unique. This is whoefully inefficient, and was the clear bottleneck in our profiles.

A less naïve approach uses a set of bits for representing literals, an `IntSet` for and-lists, and a normalized multiset for xor maps. We found more efficient to use a multiset for intermediate computations with xor maps which is normalized at the end instead of trying to track even/odd number of occurrences. Only computing Cartesian products in this representation requires some thought for finding a reasonably efficient algorithm.

While significantly faster, this was still not sufficiently efficient. Our final representation uses Natural numbers as and-maps where the encoding of literals is now positional, and xor maps are again multisets of these "bitmaps".

As a last optimization, our circuits have a very particular property: the control wires are not written to, so that they are all literals. This can be used to further optimize the evaluation of single gates.

4.3 Implementation

The final code consists of 18 modules that implement various services, see Fig. 3 for a full listing. It consists of only 1458 lines of Haskell code, of which 643 lines are blank, import or comments, module declaration, so that 815 are "code". Testing and printing utilities are not counted in the above.

The code that occupies the most volume is that for running the examples, as each circuit needs its own setup for the input and ancilla wires. Next is the implementation of symbolic representations of formulas in ANF.

TODO largest files are for running the examples, implementing formulas symbolically in ANF, code for arithmetic circuits, synthesis algorithm, and the library of algorithms.

Comment on

- `snand` being in the class instead of outside.
- `GToffoli` leaving some invariant un-expressed
- 1471 LOC, of which about $\frac{1}{3}$ is imports and comments.
- largest files are for running the examples, implementing formulas symbolically in ANF, code for arithmetic circuits, synthesis algorithm, and the library of algorithms.

5 Evaluation

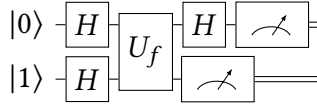
Algorithms.

We implement six well-known quantum algorithms: Deutsch, Deutsch-Jozsa, Bernstein-Vazirani, Simon, Grover, and Shor. We highlight the salient results for the first five algorithms, and then discuss the most interesting case of Shor's algorithm in detail.

De-Quantization. We abbreviate the set $\{0, 1, \dots, (n-1)\}$ as $[n]$. In the Deutsch-Jozsa problem, we are given a function $[2^n] \rightarrow [2]$ that is promised to be constant or balanced and

Module	Service
Value	representation of a <i>language of values</i> (as a typeclass) and some constructors
FormulaRepr	abstract representation of formulas, as a mapping from abstract variables to abstract formulas
Variable	variables as locations holding values and their constructors
ModularArith	modular arithmetic utilities useful in implementing certain algorithms, like Shor's
BoolUtils	function to interpret a list of booleans as an Integer
GToffoli	representation of generalized Toffoli gates and some constructors
Circuits	representation of circuits (sequences of gates) and of the special "wires" of our circuits
Synthesis	synthesis algorithm for circuits with particular properties
ArithCirc	creation of arithmetic circuits
EvalZ	evaluation of circuits on concrete values
FormAsList	representation of formulas as xor-lists of and-lists of literals-as-strings
FormAsMaps	representation of formulas as xor-maps of and-maps of literals-as-Int
FormAsBitmaps	representation of formulas as xor-maps of bitmaps
SymbEval	Symbolic evaluation of circuits
SymbEvalSpecialized	Symbolic evaluation of circuits specialized to the representation from FormAsBitmaps
QAlgos	generating the circuits themselves
RunQAlgos	running the actual circuits
Trace	utilities for tracing and debugging

Figure 3. Modules and their services

Figure 4. Quantum Circuit for the Deutsch-Jozsa Algorithm ($n = 1$)

we need to distinguish the two cases. The quantum circuit Fig. 4 shows the algorithm for the case $n = 1$. Instead of the conventional execution, we perform a retrodictive execution of the U_f block with an ancilla measurement 0, i.e., with the state $|x_{n-1} \cdots x_1 x_0 0\rangle$. The result of the execution is a symbolic formula r that determines the conditions under which $f(x_{n-1}, \dots, x_0) = 0$. When the function is constant, the results are $0 = 0$ (always) or $1 = 0$ (never). When the function is balanced, we get a formula that mentions the relevant variables. For example, here are the results of three executions for balanced functions $[2^6] \rightarrow [2]$:

- $x_0 = 0$,
- $x_0 \oplus x_1 \oplus x_2 \oplus x_3 \oplus x_4 \oplus x_5 = 0$, and
- $1 \oplus x_3 x_5 \oplus x_2 x_4 \oplus x_1 x_5 \oplus x_0 x_3 \oplus x_0 x_2 \oplus x_3 x_4 x_5 \oplus x_2 x_3 x_5 \oplus x_1 x_3 x_5 \oplus x_0 x_3 x_5 \oplus x_0 x_1 x_4 \oplus x_0 x_1 x_2 \oplus x_2 x_3 x_4 x_5 \oplus x_1 x_3 x_4 x_5 \oplus x_1 x_2 x_4 x_5 \oplus x_1 x_2 x_3 x_5 \oplus x_0 x_3 x_4 x_5 \oplus x_0 x_2 x_4 x_5 \oplus x_0 x_2 x_3 x_5 \oplus x_0 x_1 x_4 x_5 \oplus x_0 x_1 x_3 x_5 \oplus x_0 x_1 x_3 x_4 \oplus x_0 x_1 x_2 x_4 \oplus x_0 x_1 x_2 x_4 x_5 \oplus x_0 x_1 x_2 x_3 x_5 \oplus x_0 x_1 x_2 x_3 x_4 = 0$.

In the first case, the function is balanced because it produces 0 exactly when $x_0 = 0$ which happens half of the time in all possible inputs; in the second case the output of the function is the exclusive-or of all the input variables which is another easy instance of a balanced function. The last case is

a cryptographically strong balanced function whose output pattern is balanced but, by design, difficult to discern [10].

An important insight is that we actually do not care about the exact formula. Indeed, since we are promised that the function is either constant or balanced, then any formula that refers to at least one variable must indicate a balanced function. In other words, the outcome of the algorithm can be immediately decided if the formula is anything other than 0 or 1. Indeed, our implementation correctly identifies all 12870 balanced functions $[2^4] \rightarrow [2]$. This is significant as some of these functions produce complicated entangled patterns during quantum evolution and could not be de-quantized using previous approaches [1]. A word of caution though: our results assume a "white-box" complexity model rather than a "black-box" complexity model [24].

The discussion above suggests that the details of the equations may not be particularly relevant for some algorithms. This would be crucial as the satisfiability of general boolean equations is, in general, an NP-complete problem [12, 21, 31]. Fortunately, this observation does hold for other algorithms as well including the Bernstein-Vazirani algorithm and Grover's algorithm. In both cases, the result can be immediately read from the formula. In the Bernstein-Vazirani case, formulae are guaranteed to be of the form $x_1 \oplus x_3 \oplus x_4 \oplus x_5$; the secret string is then the binary number that has a 1 at the indices of the relevant variables $\{1, 3, 4, 5\}$. In the case for Grover, because there is a unique input u for which $f(u) = 1$, the ANF formula must include a subformula matching the binary representation of u , and in fact that subformula is guaranteed to be the shortest one as shown in Fig. 5.

$$\begin{aligned}
 u = 0 & \quad \mathbf{1} \oplus x_3 \oplus x_2 \oplus x_1 \oplus x_0 \oplus x_2x_3 \oplus x_1x_3 \oplus x_1x_2 \oplus x_0x_3 \oplus x_0x_2 \oplus x_0x_1 \oplus x_1x_2x_3 \oplus x_0x_2x_3 \\
 & \quad \oplus x_0x_1x_3 \oplus x_0x_1x_2 \oplus x_0x_1x_2x_3 \\
 u = 1 & \quad \mathbf{x_0} \oplus x_0x_3 \oplus x_0x_2 \oplus x_0x_1 \oplus x_0x_2x_3 \oplus x_0x_1x_3 \oplus x_0x_1x_2 \oplus x_0x_1x_2x_3 \\
 u = 2 & \quad \mathbf{x_1} \oplus x_1x_3 \oplus x_1x_2 \oplus x_0x_1 \oplus x_1x_2x_3 \oplus x_0x_1x_3 \oplus x_0x_1x_2 \oplus x_0x_1x_2x_3 \\
 u = 3 & \quad \mathbf{x_0x_1} \oplus x_0x_1x_3 \oplus x_0x_1x_2 \oplus x_0x_1x_2x_3 \\
 u = 4 & \quad \mathbf{x_2} \oplus x_2x_3 \oplus x_1x_2 \oplus x_0x_2 \oplus x_1x_2x_3 \oplus x_0x_2x_3 \oplus x_0x_1x_2 \oplus x_0x_1x_2x_3 \\
 u = 5 & \quad \mathbf{x_0x_2} \oplus x_0x_2x_3 \oplus x_0x_1x_2 \oplus x_0x_1x_2x_3 \\
 u = 6 & \quad \mathbf{x_1x_2} \oplus x_1x_2x_3 \oplus x_0x_1x_2 \oplus x_0x_1x_2x_3 \\
 u = 7 & \quad \mathbf{x_0x_1x_2} \oplus x_0x_1x_2x_3 \\
 u = 8 & \quad \mathbf{x_3} \oplus x_2x_3 \oplus x_1x_3 \oplus x_0x_3 \oplus x_1x_2x_3 \oplus x_0x_2x_3 \oplus x_0x_1x_3 \oplus x_0x_1x_2x_3 \\
 u = 9 & \quad \mathbf{x_0x_3} \oplus x_0x_2x_3 \oplus x_0x_1x_3 \oplus x_0x_1x_2x_3 \\
 u = 10 & \quad \mathbf{x_1x_3} \oplus x_1x_2x_3 \oplus x_0x_1x_3 \oplus x_0x_1x_2x_3 \\
 u = 11 & \quad \mathbf{x_0x_1x_3} \oplus x_0x_1x_2x_3 \\
 u = 12 & \quad \mathbf{x_2x_3} \oplus x_1x_2x_3 \oplus x_0x_2x_3 \oplus x_0x_1x_2x_3 \\
 u = 13 & \quad \mathbf{x_0x_2x_3} \oplus x_0x_1x_2x_3 \\
 u = 14 & \quad \mathbf{x_1x_2x_3} \oplus x_0x_1x_2x_3 \\
 u = 15 & \quad \mathbf{x_0x_1x_2x_3}
 \end{aligned}$$

Figure 5. Result of retrodictive execution for the Grover oracle ($n = 4$, w in the range $\{0..15\}$). The highlighted red subformula is the binary representation of the hidden input u .

Base	Equations	Solution
$a = 11$	$x_0 = 0$	$\mathbf{x_0 = 0}$
$a = 4, 14$	$1 \oplus x_0 = 1$	$\mathbf{x_0 = 0}$
$a = 7, 13$	$1 \oplus x_1 \oplus x_0x_1 = 1$	$\mathbf{x_0 = x_1 = 0}$
$a = 2, 8$	$1 \oplus x_0 \oplus x_1 \oplus x_0x_1 = 1$	$\mathbf{x_0 = x_1 = 0}$

Figure 6. Equations generated by retrodictive execution of $a^x \bmod 15$ for different values of a , starting from observed result 1 and unknown $x_8x_7x_6x_5x_4x_3x_2x_1x_0$. The solution for the unknown variables is given in the last column.

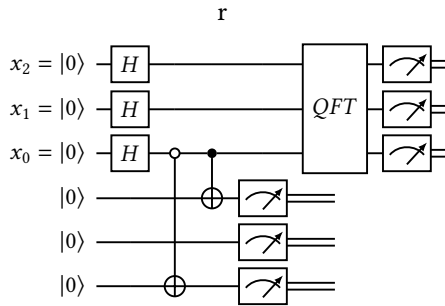


Figure 7. Finding the period of $4^x \bmod 15$

Shor's Algorithm. The circuit in Fig. 7 uses a hand-optimized implementation of quantum oracle U_f for the modular exponentiation function $f(x) = 4^x \bmod 15$ to factor 15 using Shor's algorithm. The white dot in the graphical representation of the first indicates that the control is active when it is 0. In a conventional forward execution, the state before the

QFT block is:

$$\frac{1}{2\sqrt{2}} ((|0\rangle + |2\rangle + |4\rangle + |6\rangle) |1\rangle + (|1\rangle + |3\rangle + |5\rangle + |7\rangle) |4\rangle)$$

At this point, the ancilla register is measured to either $|1\rangle$ or $|4\rangle$. In either case, the computational register snaps to a state of the form $\sum_{r=0}^3 |a + 2r\rangle$ whose QFT has peaks at $|0\rangle$ or $|4\rangle$ making them the most likely outcomes of measurements of the computational register. If we measure $|0\rangle$, we repeat the experiment; otherwise we infer that the period is 2.

In the retrodictive execution, we can start with the state $|x_2x_1x_0001\rangle$ since 1 is guaranteed to be a possible ancilla measurement (corresponding to $f(0)$). The first cx-gate changes the state to $|x_2x_1x_0x_001\rangle$ and the second cx-gate produces $|x_2x_1x_0x_00x_0\rangle$. At that point, we reconcile the retrodictive result of the ancilla register $|x_00x_0\rangle$ with the initial condition $|000\rangle$ to conclude that $x_0 = 0$. In other words, in order to observe the ancilla at 001, the computational register must be initialized to a superposition of the form $|??0\rangle$ where the least significant bit must be 0 and the other two bits are unconstrained. Expanding the possibilities, the first register needs to be in a superposition of the states $|000\rangle, |010\rangle, |100\rangle$

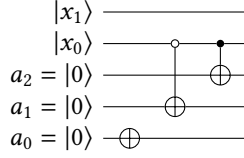


Figure 8. Finding the period of $4^x \bmod 21$ using qutrits. The three gates are from left to right are the X, SUM, and $C(X)$ gates for ternary arithmetic [8]. The X gate adds 1 modulo 3; the controlled version $C(X)$ only increments when the control is equal to 2, and the SUM gates maps $|a, b\rangle$ to $|a, a + b\rangle$.

or $|110\rangle$ and we have just inferred using purely classical but retrodictive reasoning that the period is 2.

This result does not, in fact, require the small optimized circuit of Fig. 7. In our implementation, modular exponentiation circuits are constructed from first principles using adders and multipliers [32]. In the case of $f(x) = 4^x \bmod 15$, although the unoptimized constructed circuit has 56,538 generalized Toffoli gates (controlledⁿ-not gates for all n), the execution results in just two simple equations: $x_0 = 0$ and $1 \oplus x_0 = 1$. Furthermore, as shown in Fig. 6, the shape and size of the equations is largely insensitive to the choice of 4 as the base of the exponent, leading in all cases to the immediate conclusion that the period is either 2 or 4. When the solution is $x_0 = 0$, the period is 2, and when it is $x_0 = x_1 = 0$, the period is 4.

The remarkable effectiveness of retrodictive computation of the Shor instance for factoring 15 is due to a coincidence: a period that is a power of 2 is clearly trivial to represent in the binary number system which, after all is expressly designed for that purpose. That coincidence repeats itself when factoring products of the (known) Fermat primes: 3, 5, 17, 257, and 65537, and leads to small circuits [16]. This is confirmed with our implementation which smoothly deals with unoptimized circuits for factoring such products. Factoring $3 \cdot 17 = 51$ using the unoptimized circuit of 177,450 generalized Toffoli gates produces just the 4 equations: $1 \oplus x_1 = 1$, $x_0 = 0$, $x_0 \oplus x_0 x_1 = 0$, and $x_1 \oplus x_0 x_1 = 0$. Even for $3 \cdot 65537 = 196611$ whose circuit has 4,328,778 generalized Toffoli gates, the execution produces 16 small equations that refer to just the four variables x_0, x_1, x_2 , and x_3 constraining them to be all 0, i.e., asserting that the period is 16.

Since periods that are powers of 2 are rare and special, we turn our attention to factoring problems with other periods. The simplest such problem is that of factoring 21 with an underlying function $f(x) = 4^x \bmod 21$ of period 3. The unoptimized circuit constructed from the first principles has 78,600 generalized Toffoli gates; its execution generates just three equations. But even in this rather trivial situation, the equations span 5 pages of text! (Supplementary Material). A small optimization reducing the number of qubits results

in a circuit of 15,624 generalized Toffoli gates whose execution produces still quite large, but more reasonable, equations (Supplementary Material). To understand the reason for these unwieldy equations, we examine a general ANF formula of the form $X_1 \oplus X_2 \oplus X_3 \oplus \dots = 0$ where each X_i is a conjunction of some boolean variables, i.e., the variables in each X exhibit constructive interference as they must all be true to enable that $X = 1$. Since the entire formula must equal to 0, every $X_i = 1$ must be offset by another $X_j = 1$, thus exhibiting negative interference among X_i and X_j . Generally speaking, arbitrary interference patterns can be encoded in the formulae at the cost of making the size of the formulae exponential in the number of variables. This exponential blowup is actually a necessary condition for any quantum algorithm that can offer an exponential speed-up over classical computation [20].

It would however be incorrect to conclude that factoring 21 is inherently harder than factoring 15. The issue is simply that the binary number system is well-tuned to expressing patterns over powers of 2 but a very poor match for expressing patterns over powers of 3. Indeed, we show that by just using qutrits, the circuit and equations for factoring 21 become trivial while those for factoring 15 become unwieldy. The manually optimized circuit in Fig. 8 consists of just three gates; its retrodictive execution produces two equations: $x_0 = 0$ and $x_0 \neq 2$, setting $x_0 = 0$ and leaving x_1 unconstrained. The matching values in the qutrit system as 00, 10, 20 or in decimal 0, 3, 6 clearly identifying the period to be 3. The idea of adapting the computation to simplify the circuit and equations is inspired by the fact that entanglement is relative to a particular tensor product decomposition (Methods).

6 Conclusion

7 Old

Quantum evolution is time-reversible and yet little advantage is gained from this fact in the circuit model of quantum computing. Indeed, most quantum algorithms expressed in the circuit model compute strictly from the present to the future, preparing initial states and proceeding forward with unitary transformations and measurements. In contrast, retrodictive quantum theory [5], retrocausality [2], and the time-symmetry of physical laws [33] all suggest that quantum computation embodies richer –untapped– modes of computation, which could exploit knowledge about the future for a computational advantage.

Here we demonstrate that, in concert with the computational concepts of demand-driven lazy evaluation [18] and symbolic partial evaluation [15], retrodictive reasoning can indeed be used as a computational resource that exhibits richer modes of computation at the boundary of the classical/quantum divide. Specifically, instead of fully specifying the initial conditions of a quantum circuit and computing

forward, it is possible to compute, classically, in both the forward and backward directions starting from partially specified initial and final conditions. Furthermore, this mixed mode of computation (i) can solve problems with fewer resources than the conventional forward mode of execution, sometimes even purely classically, (ii) can be expressed in a symbolic representation that immediately exposes global properties of the wavefunction that are needed for quantum algorithms, (iii) can lead to the de-quantization of some quantum algorithms, providing efficient classical algorithms inspired by their quantum counterparts, and (iv) reveals that the entanglement patterns inherent in genuine quantum algorithms with no known classical counterparts are artifacts of the chosen symbolic representation.

The main ideas underlying our contributions can be illustrated with the aid of the small examples in Fig. 9. In the conventional computational mode (Fig. 9a), the execution starts with the initial state $|00\rangle$. The first gate (Hadamard) evolves the state to $1/\sqrt{2}(|00\rangle + |10\rangle)$ which is transformed by the controlled-not (cx) gate to $1/\sqrt{2}(|00\rangle + |11\rangle)$. The measurements at the end produce 00 or 11 with equal probability. Fig. 9b keeps the quantum core of the circuit, removing the measurements, and naming the inputs and outputs with symbolic variables. Now, instead of setting $x_1 = y_1 = 0$ and computing forward as before, we can, for example, set $x_2 = 1$ and $y_2 = 0$ and calculate backwards as follows: $|10\rangle$ evolves in the backwards direction to $|11\rangle$ and then to $1/\sqrt{2}(|01\rangle - |11\rangle)$. In other words, in order to observe $x_2 y_2 = 10$, the variable x_1 should be prepared in the superposition $1/\sqrt{2}(|0\rangle - |1\rangle)$ and y_1 should be prepared in the state $|1\rangle$. More interestingly, we can partially specify the initial and final conditions. For example, we can fix $x_1 = 0$ and $x_2 = 1$ and ask if there

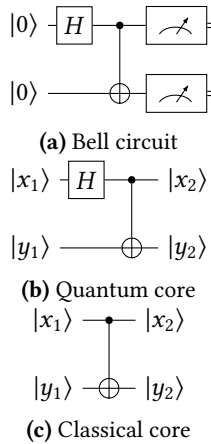


Figure 9. A conventional quantum circuit with initial conditions and measurement (a); its quantum core without measurement and with unspecified initial and final conditions (b); and its classical core without explicit quantum superpositions (c).

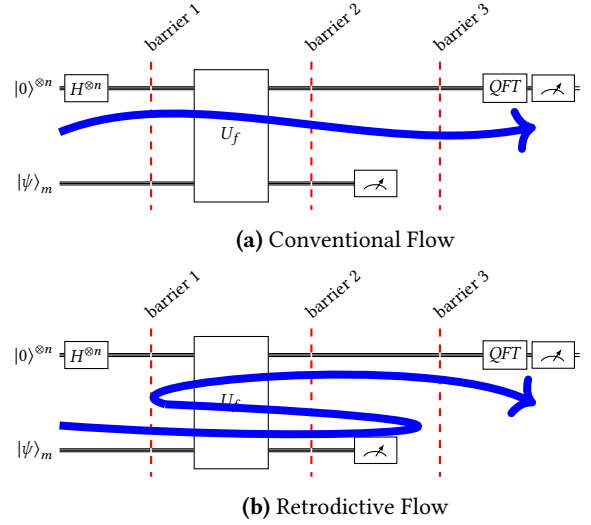


Figure 10. Template quantum circuit

are any possible values for y_1 and y_2 that would be consistent with this setting. To answer the question, we calculate, using the techniques of symbolic partial evaluation (Methods), as follows. The initial state is $|0y_1\rangle$ which evolves to $1/\sqrt{2}(|0y_1\rangle + |1y_1\rangle)$ and then to $1/\sqrt{2}(|0y_1\rangle + |1(1 \oplus y_1)\rangle)$ where \oplus is the exclusive-or operation and $1 \oplus y_1$ is the canonical way of negating y_1 in the Algebraic Normal Form (ANF) of boolean expressions (Methods). This final state can now be reconciled with the specified final conditions $1y_2$ revealing that the settings are consistent provided that $y_2 = 1 \oplus y_1$. We can, in fact, go one step further and analyze the circuit without the Hadamard gate as shown in Fig. 9c. The reasoning is that the role of Hadamard is to introduce (modulo phase) uncertainty about whether $x_1 = 0$ or $x_1 = 1$. But, again modulo phase, the same uncertainty can be expressed by just using the variable x_1 . Thus, in Fig. 9c, we can set $y_1 = 0$ and $y_2 = 1$ and ask about values of x_1 and x_2 that would be consistent with this setting. We can calculate backwards from $|x_2 1\rangle$ as follows. The state evolves to $|x_2(1 \oplus x_2)\rangle$ which can be reconciled with the initial conditions yielding the constraints $x_1 = x_2$ and $1 \oplus x_2 = 0$ whose solutions are $x_1 = x_2 = 1$.

These insights are robust and can be implemented in software (Methods) to analyze circuits with millions of gates for the quantum algorithms that match the template in Fig. 10 (including Deutsch, Deutsch-Jozsa, Bernstein-Vazirani, Simon, Grover, and Shor's algorithms [7, 13, 14, 17, 26, 28, 29]). The software is completely classical, performing mixed mode executions of the classical core of the circuits, i.e., the U_f block defined as $U_f(|x\rangle|y\rangle) = |x\rangle|f(x) \oplus y\rangle$. Specifically, in all these algorithms, the top collection of wires (which we will call the computational register) is prepared in a uniform superposition which can be represented using symbolic variables. The measurement of the bottom collection of wires (which we call the ancilla register) after barrier 2 provides

partial information about the future which is, together with the initial conditions of the ancilla register, sufficient to symbolically execute the circuit. In each case, instead of the conventional execution flow depicted in Fig. 10(a), we find a possible measurement outcome w at barrier (2) and perform a symbolic retrodictive execution with a state $|xw\rangle$ going backwards to collect the constraints on x that enable us to solve the problem in question.

Methods

Symbolic Execution of Classical Programs. A well-established technique to simultaneously explore multiple paths that a classical program could take under different inputs is *symbolic execution* [4, 9, 11, 19, 22]. In this execution scheme, concrete values are replaced by symbols which are initially unconstrained. As the execution proceeds, the symbols interact with program constructs and this typically introduces constraints on the possible values that the symbols represent. At the end of the execution, these constraints can be solved to infer properties of the program under consideration.

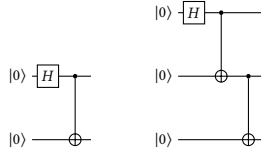


Figure 11. Bell and GHZ States

Entanglement. A symbolic variable represents a boolean value that can be 0 or 1; this is similar to a qubit in a superposition $(1/\sqrt{2})(|0\rangle \pm |1\rangle)$. Thus, it appears that $H|0\rangle$ could be represented by a symbol x to denote the uncertainty. Surprisingly, this idea scales to even represent maximally entangled states. Fig. 11 (left) shows a circuit to generate the Bell state $(1/\sqrt{2})(|00\rangle + |11\rangle)$. By using the symbol x for $H|0\rangle$, the input to the cx-gate is $|x0\rangle$ which evolves to $|xx\rangle$. By sharing the same symbol in two positions, the symbolic state accurately represents the entangled Bell state. Similarly, for the circuit in Fig. 11 (right), the state after the Hadamard gate is $|x00\rangle$ which evolves to $|xx0\rangle$ and then to $|xxx\rangle$ again accurately capturing the entanglement correlations.

Given a maximally entangled state defined with respect to a particular tensor product decomposition, the same state may become unentangled in a different tensor product decomposition. Given the state:

$$|\Psi\rangle = |0\rangle + |3\rangle + |6\rangle + |9\rangle + |12\rangle + |15\rangle,$$

one can find a 4-qubit representation ($\mathcal{H} = \bigotimes_{i=1}^4 \mathbb{C}^2$)

$$|\Psi\rangle = |0000\rangle + |0011\rangle + |0110\rangle + |1001\rangle + |1100\rangle + |1111\rangle,$$

where we used the following map $|m\rangle = \sum_{i=0}^3 x_i 2^i$, with $m \in \mathbb{Z}$ and $x_i = 0, 1$. One can use the purity [6]

$$P_{|\Psi\rangle} = \frac{1}{4} \sum_{i=1}^4 \sum_{\mu=x,y,z} \langle \Psi | \sigma_i^\mu | \Psi \rangle^2$$

and confirm that the state $|\Psi\rangle$ is maximally entangled, i.e., has $P_{|\Psi\rangle} = 0$. In contrast, in a qutrit basis ($\mathcal{H} = \bigotimes_{i=1}^4 \mathbb{C}^3$), given the map $|m\rangle = \sum_{i=0}^2 x_i 3^i$, with $x_i = 0, 1, 2$, the state

$$\begin{aligned} |\Psi\rangle &= |0000\rangle + |0010\rangle + |0020\rangle + |0100\rangle + |0110\rangle + |0120\rangle \\ &= |0\rangle \otimes (|0\rangle + |1\rangle) \otimes (|0\rangle + |1\rangle + |2\rangle) \otimes |0\rangle, \end{aligned}$$

is a product (unentangled) state.

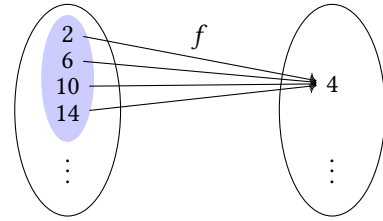


Figure 12. The pre-image of 4 under $f(x) = 7^x \bmod 15$.

Complexity Analysis. Given finite sets A and B , a function $f : A \rightarrow B$ and an element $y \in B$, we define $\{\cdot \xleftarrow{f} y\}$, the pre-image of y under f , as the set $\{x \in A \mid f(x) = y\}$. For example, let $A = B = [2^4]$ and let $f(x) = 7^x \bmod 15$, then the collection of values that f maps to 4, $\{\cdot \xleftarrow{f} 4\}$, is the set $\{2, 6, 10, 14\}$ as shown in Fig. 12. Symbolic retrodictive execution can be seen as a method to generate boolean formulae that describe the pre-image of the function f under study. For the example in Fig. 12, retrodictive execution might generate the formulae $x_1 = 1$ and $x_0 = 0$. The (trivial in this case) solution for the formulae is indeed the set $\{2, 6, 10, 14\}$. The critical points to note, however, are that: (i) solving the equations describing the pre-image is in general an intractable (even for quantum computers) *NP*-complete problem, and (ii) solving the equations is not needed for typical quantum algorithms. *Only some global properties of the pre-image are needed!* Indeed, we have already seen that for solving the Deutsch-Jozsa problem, the only thing needed was whether the formula contains some variables. For the Bernstein-Vazirani problem, the only thing needed was the indices of the variables occurring in the formula. For Grover's algorithm, we only need to extract the singleton element in the pre-image and for Shor's algorithm we "only" need to extract the periodicity of the elements in the pre-image.

To appreciate the difficulty of computing pre-images in general, note that finding the pre-image of a function subsumes several challenging computational problems such as pre-image attacks on hash functions [27], predicting environmental conditions that allow certain reactions to take place

in computational biology [3, 23], and finding the pre-image of feature vectors in the space induced by a kernel in neural networks [25]. More to the point, the boolean satisfiability problem SAT is expressible as a boolean function over the input variables and solving a SAT problem is asking for the pre-image of true. Indeed, based on the conjectured existence of one-way functions which itself implies $P \neq NP$, all these pre-images calculations are believed to be computationally intractable in their most general setting.

The bottleneck in retrodictive execution, as we presented it, is therefore in the symbolic execution of circuits in the ANF domain. Not only does the execution scale with the number of gates in the circuit but also with the size of the intermediate ANF formulae, which could become exponential in the number of variables.

Software. The entire suite of programs including synthesis of reversible circuits, standard evaluation, retrodictive evaluation under various modes, testing, debugging, and alternative representations off ANF formulae is only 1,500 lines of Haskell. The heart of the implementation is this simple function:

```
peG :: Value v => GToffoli s v -> ST s ()
peG (GToffoli bs cs t) = do
  controls <- mapM readSTRef cs
  tv <- readSTRef t
  let funs = map (\b -> if b then id else snot) bs
  let r = sxor tv (foldr sand one (zipWith ($) funs controls))
  writeSTRef t r
```

The function performs symbolic evaluation of one generalized Toffoli gates, reading the current ANF formulae for each control and producing an appropriate ANF formula for the target.

Supplementary Information. The equations generated by retrodictive execution of the optimized circuit for $4^x \bmod 21$ starting from observed result 1 and unknown x are:

$$1 \oplus x_0 \oplus x_1 \oplus x_2 \oplus x_0 x_2 \oplus x_0 x_1 x_2 \oplus x_3 \oplus x_1 x_3 \oplus x_0 x_1 x_3 \oplus x_0 x_2 x_3 \oplus x_1 x_2 x_3 \oplus x_4 \oplus x_0 x_4 \oplus x_0 x_1 x_4 \oplus x_2 x_4 \oplus x_1 x_2 x_4 \oplus x_0 x_1 x_2 x_4 \oplus x_0 x_3 x_4 \oplus x_1 x_3 x_4 \oplus x_2 x_3 x_4 \oplus x_0 x_2 x_3 x_4 \oplus x_0 x_1 x_2 x_3 x_4 \oplus x_5 \oplus x_1 x_5 \oplus x_0 x_1 x_5 \oplus x_0 x_2 x_5 \oplus x_1 x_2 x_5 \oplus x_3 x_5 \oplus x_0 x_3 x_5 \oplus x_0 x_1 x_3 x_5 \oplus x_2 x_3 x_5 \oplus x_1 x_2 x_3 x_5 \oplus x_0 x_1 x_2 x_3 x_5 \oplus x_0 x_4 x_5 \oplus x_1 x_4 x_5 \oplus x_2 x_4 x_5 \oplus x_0 x_2 x_4 x_5 \oplus x_0 x_1 x_2 x_4 x_5 \oplus x_3 x_4 x_5 \oplus x_1 x_3 x_4 x_5 \oplus x_0 x_1 x_3 x_4 x_5 \oplus x_0 x_2 x_3 x_4 x_5 \oplus x_1 x_2 x_3 x_4 x_5 = 1$$

$$x_1 \oplus x_0 x_1 \oplus x_0 x_2 \oplus x_1 x_2 \oplus x_3 \oplus x_0 x_3 \oplus x_0 x_1 x_3 \oplus x_2 x_3 \oplus x_1 x_2 x_3 \oplus x_0 x_1 x_2 x_3 \oplus x_0 x_4 \oplus x_1 x_4 \oplus x_2 x_4 \oplus x_0 x_2 x_4 \oplus x_0 x_1 x_2 x_4 \oplus x_3 x_4 \oplus x_1 x_3 x_4 \oplus x_0 x_1 x_3 x_4 \oplus x_0 x_2 x_3 x_4 \oplus x_1 x_2 x_3 x_4 \oplus x_5 \oplus x_0 x_5 \oplus x_0 x_1 x_5 \oplus x_2 x_5 \oplus x_1 x_2 x_5 \oplus x_0 x_1 x_2 x_5 \oplus x_0 x_3 x_5 \oplus x_1 x_3 x_5 \oplus x_2 x_3 x_5 \oplus x_0 x_2 x_3 x_5 \oplus x_0 x_1 x_2 x_3 x_5 \oplus x_4 x_5 \oplus x_1 x_4 x_5 \oplus x_0 x_1 x_4 x_5 \oplus x_0 x_2 x_4 x_5 \oplus x_1 x_2 x_4 x_5 \oplus x_3 x_4 x_5 \oplus x_0 x_3 x_4 x_5 \oplus x_0 x_1 x_3 x_4 x_5 \oplus x_2 x_3 x_4 x_5 \oplus x_1 x_2 x_3 x_4 x_5 \oplus x_0 x_1 x_2 x_3 x_4 x_5 = 0$$

$$x_0 \oplus x_0 x_1 \oplus x_2 \oplus x_1 x_2 \oplus x_0 x_1 x_2 \oplus x_0 x_3 \oplus x_1 x_3 \oplus x_0 x_2 x_3 \oplus x_0 x_2 x_3 \oplus x_0 x_1 x_2 x_3 \oplus x_4 \oplus x_1 x_4 \oplus x_0 x_1 x_4 \oplus x_0 x_2 x_4 \oplus x_1 x_2 x_4 \oplus x_3 x_4 \oplus x_0 x_3 x_4 \oplus x_0 x_1 x_3 x_4 \oplus x_2 x_3 x_4 \oplus x_1 x_2 x_3 x_4 \oplus x_0 x_1 x_2 x_3 x_4 \oplus x_0 x_5 \oplus x_1 x_5 \oplus x_2 x_5 \oplus x_0 x_2 x_5 \oplus x_0 x_1 x_2 x_5 \oplus x_3 x_5 \oplus x_1 x_3 x_5 \oplus x_0 x_1 x_3 x_5 \oplus x_0 x_2 x_3 x_5 \oplus x_1 x_2 x_3 x_5 \oplus x_4 x_5 \oplus x_0 x_4 x_5 \oplus x_0 x_1 x_4 x_5 \oplus x_2 x_4 x_5 \oplus x_1 x_2 x_4 x_5 \oplus x_0 x_1 x_2 x_4 x_5 \oplus x_0 x_3 x_4 x_5 \oplus x_1 x_3 x_4 x_5 \oplus x_2 x_3 x_4 x_5 \oplus x_0 x_2 x_3 x_4 x_5 \oplus x_0 x_1 x_2 x_3 x_4 x_5 = 0$$

The equations generated by retrodictive execution of the unoptimized $4^x \bmod 21$ starting from observed result 1 and unknown x . The circuit consists of 36,400 cx-gates, 38,200 ccx-gates, and 4,000 cccx-gates. There are only three equations but each equation is exponentially large.

References

- [1] ABBOTT, A. A. The Deutsch-Jozsa problem: de-quantization and entanglement. *Natural Computing* 11 (2012).
- [2] AHARONOV, Y., AND VAIDMAN, L. *The Two-State Vector Formalism: An Updated Review*. Springer Berlin Heidelberg, Berlin, Heidelberg, 2008, pp. 399–447.
- [3] AKUTSU, T., HAYASHIDA, M., ZHANG, S.-Q., CHING, W.-K., AND NG, M. K. Analyses and algorithms for predecessor and control problems for boolean networks of bounded indegree. *Information and Media Technologies* 4, 2 (2009), 338–349.
- [4] BALDONI, R., COPPA, E., D’ELIA, D. C., DEMETRESCU, C., AND FINOCCHI, I. A survey of symbolic execution techniques. *ACM Comput. Surv.* 51, 3 (may 2018).
- [5] BARNETT, S. M., JEFFERS, J., AND PEGG, D. T. Quantum retrodiction: Foundations and controversies. *Symmetry* 13, 4 (2021).
- [6] BARNUM, H., KNILL, E., ORTIZ, G., SOMMA, R., AND VIOLA, L. A subsystem-independent generalization of entanglement. *Phys. Rev. Lett.* 92 (Mar 2004), 107902.
- [7] BERNSTEIN, E., AND VAZIRANI, U. Quantum complexity theory. *SIAM Journal on Computing* 26, 5 (1997), 1411–1473.
- [8] BOCHAROV, A., CUI, S. X., ROETTELIER, M., AND SVORE, K. M. Improved quantum ternary arithmetic. *Quantum Info. Comput.* 16, 9–10 (jul 2016), 862–884.
- [9] BOYER, R. S., ELSPAS, B., AND LEVITT, K. N. Select—a formal system for testing and debugging programs by symbolic execution. *SIGPLAN Not.* 10, 6 (apr 1975), 234–245.
- [10] BURNETT, L., MILLAN, W., DAWSON, E., AND CLARK, A. Simpler methods for generating better boolean functions with good cryptographic properties. *Australasian Journal of Combinatorics* 29 (2004), 231–247.
- [11] CLARKE, L. A. A program testing system. In *Proceedings of the 1976 Annual Conference* (New York, NY, USA, 1976), ACM ’76, Association for Computing Machinery, p. 488–491.
- [12] COOK, S. A. The complexity of theorem-proving procedures. In *Proceedings of the Third Annual ACM Symposium on Theory of Computing* (New York, NY, USA, 1971), STOC ’71, Association for Computing Machinery, p. 151–158.
- [13] DEUTSCH, D. Quantum theory, the church–turing principle and the universal quantum computer. *Proc. R. Soc. Lond. A* 400 (1985).
- [14] DEUTSCH, D., AND JOZSA, R. Rapid solution of problems by quantum computation. *Proc. R. Soc. Lond. A* 439 (1992).
- [15] FUTAMURA, Y. Partial computation of programs. In *RIMS Symposia on Software Science and Engineering* (Berlin, Heidelberg, 1983), E. Goto, K. Furukawa, R. Nakajima, I. Nakata, and A. Yonezawa, Eds., Springer Berlin Heidelberg, pp. 1–35.
- [16] GELLER, M. R., AND ZHOU, Z. Factoring 51 and 85 with 8 qubits. *Scientific Reports* (2023) 3, 1 (2013).

- [17] GROVER, L. K. A fast quantum mechanical algorithm for database search. In *Proceedings of the Twenty-Eighth Annual ACM Symposium on Theory of Computing* (New York, NY, USA, 1996), STOC '96, Association for Computing Machinery, p. 212–219.
- [18] HENDERSON, P., AND MORRIS, J. H. A lazy evaluator. In *Proceedings of the 3rd ACM SIGACT-SIGPLAN Symposium on Principles on Programming Languages* (New York, NY, USA, 1976), POPL '76, Association for Computing Machinery, p. 95–103.
- [19] HOWDEN, W. E. Experiments with a symbolic evaluation system. In *Proceedings of the National Computer Conference* (1976).
- [20] JOZA, R., AND LINDEN, N. On the role of entanglement in quantum-computational speed-up. *Proceedings: Mathematical, Physical and Engineering Sciences* 459, 2036 (2003), 2011–2032.
- [21] KARP, R. M. *Reducibility among Combinatorial Problems*. Springer US, Boston, MA, 1972, pp. 85–103.
- [22] KING, J. C. Symbolic execution and program testing. *Commun. ACM* 19, 7 (jul 1976), 385–394.
- [23] KLOTZ, J. G., BOSSERT, M., AND SCHÖBER, S. Computing preimages of boolean networks. *BMC Bioinformatics* 14, 10 (Aug 2013), S4.
- [24] KOMARGODSKI, I., NAOR, M., AND YOGEV, E. White-box vs. black-box complexity of search problems: Ramsey and graph property testing. *J. ACM* 66, 5 (jul 2019).
- [25] KWOK, J.-Y., AND TSANG, I.-H. The pre-image problem in kernel methods. *IEEE Transactions on Neural Networks* 15, 6 (2004), 1517–1525.
- [26] NIELSEN, M. A., AND CHUANG, I. L. *Quantum Computation and Quantum Information: 10th Anniversary Edition*. Cambridge University Press, 2010.
- [27] ROGAWAY, P., AND SHRIMPTON, T. Cryptographic hash-function basics: Definitions, implications, and separations for preimage resistance, second-preimage resistance, and collision resistance. In *Fast Software Encryption* (Berlin, Heidelberg, 2004), B. Roy and W. Meier, Eds., Springer Berlin Heidelberg, pp. 371–388.
- [28] SHOR, P. W. Polynomial-time algorithms for prime factorization and discrete logarithms on a quantum computer. *SIAM Journal on Computing* 26, 5 (1997), 1484–1509.
- [29] SIMON, D. On the power of quantum computation. In *Proceedings 35th Annual Symposium on Foundations of Computer Science* (1994), pp. 116–123.
- [30] TOKAREVA, N. Chapter 1 - Boolean functions. In *Bent Functions*, N. Tokareva, Ed. Academic Press, Boston, 2015, pp. 1–15.
- [31] TRAKHTENBROT, B. A survey of russian approaches to perebor (brute-force searches) algorithms. *Annals of the History of Computing* 6, 4 (1984), 384–400.
- [32] VEDRAL, V., BARENCO, A., AND EKERT, A. Quantum networks for elementary arithmetic operations. *Phys. Rev. A* 54 (Jul 1996), 147–153.
- [33] WATANABE, S. Symmetry of physical laws. Part III. prediction and retrodiction. *Rev. Mod. Phys.* 27 (Apr 1955), 179–186.
- [34] WEGENER, I. *The Complexity of Boolean Functions*. John Wiley & Sons, Inc., USA, 1987.